

# Preparation of Gold Nanoparticles Using Silver Halide Photographic Materials (10): Effect of Ascorbic Acid Concentration

Ken'ichi KUGE<sup>1</sup>, Hidetaka TOMIMATSU<sup>2</sup>, Yousuke IMAI<sup>3</sup>

**Abstract:** The formation of gold nanoparticles with the gold deposition development was investigated by altering the concentration of the gold(I) complex (AC) and ascorbic acid (AcA) solutions or their concentration ratio AC/AcA in the developer with three methods: absorption spectrum measurement, atomic absorption spectroscopy and transmission electron microscopy. Several phenomena, such as the variation in the development rates, existence of an induction period in the development rates, shift in the wavelength of maximum absorption, expansion of the band width, simultaneous formation of silver atoms, and change in the smoothness of the particle surface, were observed. These phenomena depended not only on the concentration of both solutions but significantly on their ratio. All these phenomena changed at a concentration ratio equal to unity, and it was suggested that the formation process varied at approximately this ratio. A novel process, whereby silver halide was reduced by excess AcA to form silver atoms and these atoms subsequently reduced gold ions to form gold atoms, was proposed to explain the acceleration of the development rates, the disappearance of the induction period, red-shift and expansion of the band, as well as the appearance of a rough surface on the particles.

**Key words:** Silver salt photographic materials, Gold deposition development, Gold nanoparticles, Formation mechanism, Ascorbic acid

## 1. Introduction

Up to now, we have reported the formation of gold nanoparticles *via* the gold deposition development method, which is a new approach in silver halide photography<sup>1-9</sup>. In this process, the latent image speck (LIS), which is a tiny speck of silver atoms formed on a silver halide grain by exposure, acts as a catalyst for the reduction of the monovalent gold-ion Au(I) complex (AC) in the developer to gold atom. These gold atoms are deposited on the LIS to form a gold nanoparticle<sup>10,11</sup>, wherefrom we can obtain an image composed of the gold nanoparticles.

It was considered that the formation of gold atoms proceeded through the disproportionation reaction of AC<sup>2, 12</sup>. We reported that the reaction rate increased with the concentration of AC in the developer<sup>3</sup>, and the addition of ascorbic acid (AcA) significantly accelerated the formation of gold atoms<sup>7</sup>. Moreover, using energy-dispersive X-ray spectroscopy, we reported that a small amount of silver atoms was formed through the reduction of silver halide by AcA<sup>8</sup>. Therefore, it was suggested that several reactions, such as the disproportionation reaction of AC, reduction of AC by AcA, or reduction of silver halide by AcA, were proceeding. The details, however, remained ambiguous.

The gold deposition development was mainly analyzed based on the condition that the concentration ratio of AC and AcA (AC/AcA) was constant. Upon altering this ratio, it is expected that different formation processes of gold nanoparticles will proceed; thus,

we can obtain information on the reaction mechanisms. Here, we altered not only the concentrations of AC and AcA but also their concentration ratios, and analyzed the formation process of gold nanoparticles by three methods: absorption spectrum measurement, atomic absorption spectroscopy, and transmission electron microscopy. Thereafter, we aimed to clarify the formation mechanism of gold nanoparticles.

## 2. Experimental method

The photographic emulsion used was composed of near-spherical silver iodobromide ultrafine grains with a size of 40–50 nm. This emulsion grain was the same as that used in the photographic glass plate of P5600 (Konica Minolta) for holography, although the emulsion used here was untreated with any sensitization, as in previous reports<sup>8, 9</sup>. An aqueous gelatin solution was added to this emulsion to adjust the silver to gelatin ratio, and the mixture was coated on a glass substrate to prepare dry plates. No hardening process was performed. This plate was referred to as plate A. In addition, we purchased the above-mentioned P5600 plate. This plate was produced after treating the spectral and chemical sensitizations to the emulsion, and underwent a hardening process. This plate was referred to as plate B,

Plate A was exposed with a xenon flash lamp for an exposure time of  $10^{-3}$  s. This lamp had been used in some previous reports<sup>1, 5, 8, 13-15</sup>\*, although its exposure value was unknown. Plate B was subjected to a high-intensity exposure using a sensitometer (EG&G Mark7)

Received 18th October, 2020; Accepted 5th December, 2020, Published 7th December, 2020

1 Radioisotope Research Center, Chiba University, 1-33, Yayoi-cho, Inage-ku, Chiba 263-8522, Japan

2 Graduate School of Advanced Integration Science, Chiba University, 1-33, Yayoi-cho, Inage-ku, Chiba 263-8522, Japan

3 Faculty of Engineering, Chiba University, 1-33, Yayoi-cho, Inage-ku, Chiba 263-8522, Japan

with an exposure time of  $10^{-3}$  s. The exposure value was 3.77, which represented the logarithm of the value with a unit of  $\text{cd}\cdot\text{s}/\text{m}^2$ . This value was less than the one obtained with the former xenon flash lamp upon comparing the sensitometry results. In both cases, the whole area of the plate was uniformly exposed.

Formulas of the developer for gold deposition development are shown in Table 1 for plate A and Table 2 for plate B. The formula of the developer was basically the same as before<sup>7-9)</sup>. The AcA solution in the formula was added to the developer just before development to adjust each concentration listed in Tables 1 and 2. The concentrations of AcA and sodium chloroaurate in the developer, and the ratio of both solutions were altered, while the concentration ratio of potassium thiocyanate and sodium chloroaurate was kept constant at an optimum value of 4:1<sup>6)</sup>. As plate A was not hardened, and the emulsion layer on the plate often swelled and peeled off easily during development, we added sodium sulfate to the developer as a swelling inhibitor.

Development was conducted at 20 °C for plate A to prevent peel-

ing, and at 25 °C for the hardened plate B. The development time was altered from 5 min to 72 h to obtain the development rates. Procedures in a development process, such as fixation, are shown in Table 3 for plate A and Table 4 for plate B.

The absorption spectrum of gold nanoparticles on the plate after the development treatment was measured with a visible spectrophotometer (Shimadzu, UV 2550). We searched the wavelength of the absorption maximum ( $\lambda_{\text{max}}$ ) in the range of 350–750 nm from each spectrum and obtained the maximum absorbance (Max Abs) in this range. Increasing in the maximum absorbance with the development time was evaluated as the increasing rate of the maximum absorbance.

An atomic absorption spectrometer (Varian, SpectrAcA-50/55) was used to measure the amount of gold or silver atoms formed on the plate. We cut out a certain area ( $25 \times 20 \text{ mm}^2$ ) of the plate after development, dissolved the gold nanoparticles on the plate with aqua regia, and diluted the solution appropriately. A calibration curve for gold was prepared from the solution by dissolving a gold wire with aqua regia, while that for silver was prepared from an aqueous solution of silver nitrate. Increasing in the gold or silver amount with the development time was evaluated as the formation rate of the gold or silver amount.

We observed the gold nanoparticles with an electron microscope. The samples for the observation were prepared using a previous method<sup>8)</sup>. The emulsion layer was scraped off from the plate after the development and the gelatin in the layer was decomposed by enzymes to make a suspension of gold nanoparticles. We placed a drop of this solution on a grid coated with a collodion membrane and dried to prepare samples for microscopy evaluation. These samples were observed with a transmission electron microscope (Hitachi, H-7650) to measure the particle diameters. Increasing in the particle diameter with the development time was evaluated as the growth rate of the particle size.

### 3. Experimental results

#### 3.1 Dependence on ascorbic acid concentration

Here, the AC concentration was fixed at  $1 \times 10^{-3}$  mol/L, and the AcA concentration in the developer was altered from  $1 \times 10^{-2}$  to  $1 \times 10^{-6}$  mol/L.

Gold nanoparticles generally absorb green light strongly by localized surface plasmon resonance. Figure 1 shows the AcA concentration dependence of the absorption spectrum of the layer with gold nanoparticles on plate A. When the AcA concentration was low, the spectrum showed a slightly sharp absorption in the green spectral region around 540–570 nm. This peak shifted to longer wavelength and the band became broader with increasing AcA concentration.

The increasing rate of the maximum absorbance is shown in Figure 2. At a low AcA concentration, the rate was low and there was an induction period, revealing a very small increase at the beginning of development. Therefore, the increase exhibited an S-shaped curve. The rate accelerated significantly with increasing AcA concentration. A significant increase in the rate and the disappearance of the induction period were observed between AcA concentrations of  $1 \times 10^{-4}$  mol/L and  $1 \times 10^{-3}$  mol/L. A significant acceleration of the

Table 1

Formula of gold deposition development for plate A (mol/L)	
KSCN	$2 \times 10^{-4} - 8 \times 10^{-3}$
$\text{NaAuCl}_4 \cdot 2\text{H}_2\text{O}$	$5 \times 10^{-5} - 2 \times 10^{-3}$
KBr	$8 \times 10^{-3}$
$\text{Na}_2\text{SO}_4$	$2 \times 10^{-2}$
Ascorbic acid	$1 \times 10^{-6} - 2 \times 10^{-3}$

Table 2

Formula of gold deposition development for plate B (mol/L)	
KSCN	$4 \times 10^{-3}$
$\text{NaAuCl}_4 \cdot 2\text{H}_2\text{O}$	$1 \times 10^{-3}$
KBr	$8 \times 10^{-3}$
Ascorbic acid	$1 \times 10^{-6} - 1 \times 10^{-2}$

Table 3

Procedure of gold deposition development for plate A Treatment temperature = 20 °C		
Development	Developer in Table 1	5 min–72 h
Stop	Pure water	5 min
Stop	Pure water	5 min
Fix	F-5 fixer	10 min
Wash	Running water	30 min
Wash	Pure water	10 min

Table 4

Procedure of gold-deposition development for plate B Treatment temperature = 25 °C		
Development	Developer in Table 2	5 min–24 h
Stop	Pure water	5 min
Stop	Pure water	5 min
Fix	F-5 fixer	10 min
Wash	Running water	30 min
Wash	Pure water	10 min

rate appeared at the initial stage with the disappearance of this induction period.

The formation rate of the gold amount ( $M_{Au}$ ) measured with atomic absorption spectrometry for plate B is shown in Figure 3. The upper figure shows the changes on a long time-scale, while the lower one presents the changes on a short time scale around the initial increase. At a low AcA concentration, the formation rate was

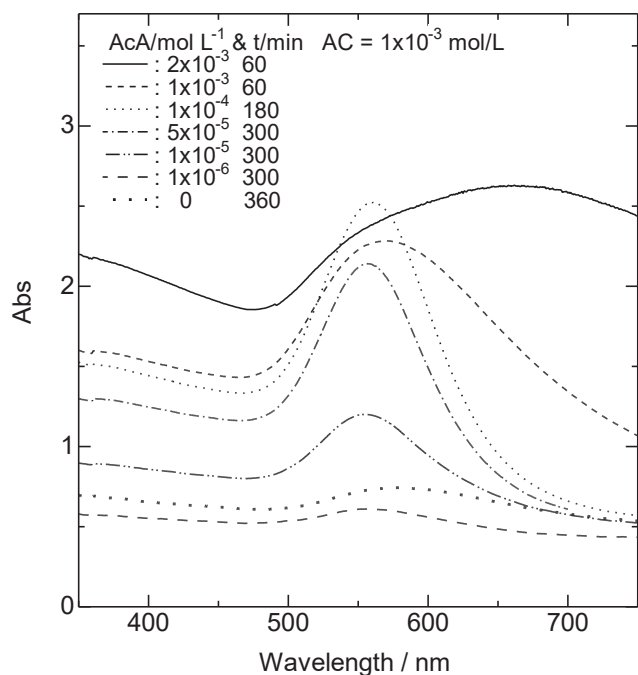


Fig. 1 Absorption spectra of gold nanoparticles formed on plate A at different concentrations of ascorbic acid (AcA) from 0 to  $2 \times 10^{-3}$  mol/L in the developer. The concentration of Au(I) complex (AC) was fixed to  $1 \times 10^{-3}$  mol/L. The development time is presented with each legend.

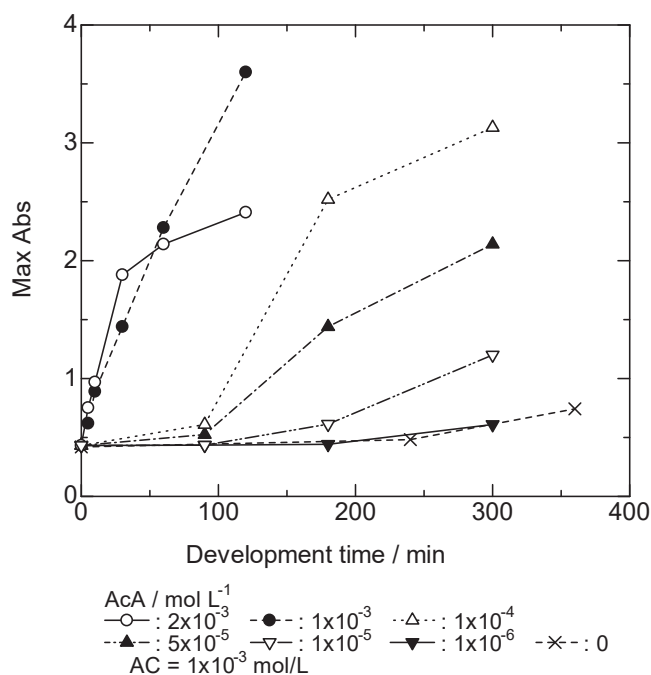


Fig. 2 Increasing rate of maximum absorbance in each spectrum of gold nanoparticles formed on plate A. The concentration of ascorbic acid (AcA) in the developer was altered from 0 to  $2 \times 10^{-3}$  mol/L, while that of Au(I) complex (AC) was fixed to  $1 \times 10^{-3}$  mol/L.

low, indicating an S-shaped curve with the induction period. The rate accelerated rapidly and the induction period became shorter with increasing AcA concentration. When the concentration exceeded  $1 \times 10^{-3}$  mol/L, the induction period almost disappeared.

The formation rate of the silver amount ( $M_{Ag}$ ) measured with atomic absorption spectrometry for plate B is shown in Fig. 4. There was almost no increase, or possibly a very small increase in the amount of silver up to an AcA concentration of  $1 \times 10^{-3}$  mol/L, while there was a sharp increase in the amount at an AcA concentration of  $1 \times 10^{-2}$  mol/L. Silver atoms were produced quickly at a high AcA concentration as described in the previous report<sup>8)</sup>, although the silver amount was approximately 1/10 of the gold one produced at the same time.

### 3.2 Dependence on gold(I) ion complex concentration

The AcA concentration was fixed at  $1 \times 10^{-4}$  mol/L or  $1 \times 10^{-3}$  mol/L for this evaluation. The AC concentration in the developer was altered from  $2 \times 10^{-3}$  to  $5 \times 10^{-5}$  mol/L. Plate A was used for the experiments in this evaluation.

#### 3.2.1 Ascorbic acid concentration of $1 \times 10^{-4}$ mol/L

The dependence of absorption spectrum on the AC concentration is shown in Figure 5. When the AC concentration was equal to or lower than the AcA concentration, the band was broad. The band

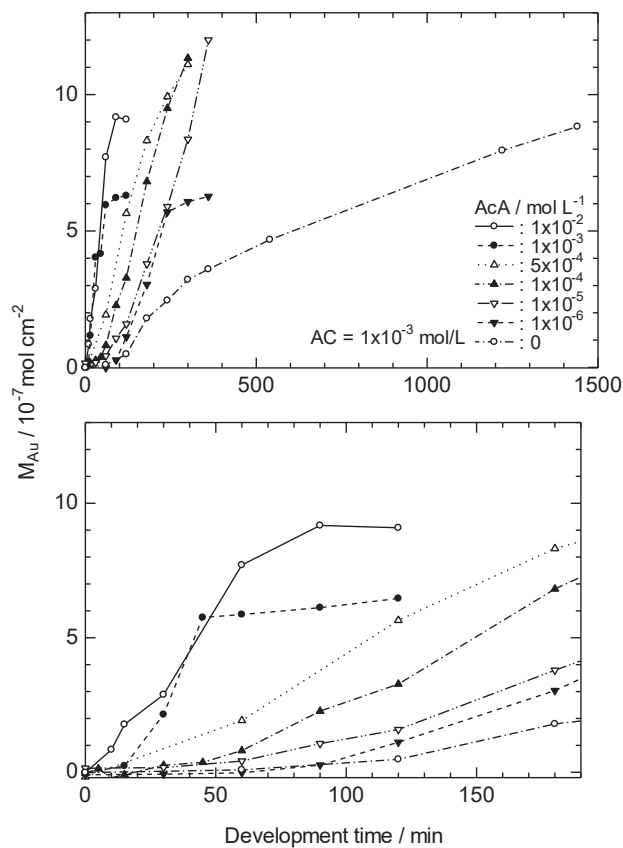


Fig. 3 Formation rate of gold amount formed on plate B measured with atomic absorption spectroscopy. The concentration of ascorbic acid (AcA) in the developer was altered from 0 to  $1 \times 10^{-2}$  mol/L, while that of Au(I) complex (AC) was fixed to  $1 \times 10^{-3}$  mol/L. Top figure: long timescale, bottom figure: short timescale highlighting the initial increase.

became sharp with an increase in AC concentration, while the wavelength of the absorption maximum did not vary as much.

The dependence of increasing rate of maximum absorbance on the AC concentration is shown in Figure 6. At a low AC concentration, there was no induction period and the initial rate was high, while the absorbance was saturated at a small value. With an increase in AC concentration, the initial rate decreased and the induction period appeared at an AC concentration of approximately  $1 \times 10^{-3}$  mol/L. The absorbance was not saturated on the experimental time scale. However, when the AcA concentration was zero, the induction period was long and the rate was extremely low. The dif-

ference in the rates with and without AcA was remarkable.

The formation rate of the gold amount measured with atomic absorption spectrometry is shown in Figure 7. At a low AC concentration, the initial rate was high and no induction period was observed. The induction period appeared and became longer along with increasing AC concentration. When the AcA concentration was zero, the induction period was long and the rate became much lower.

The growth rate of the diameter of gold nanoparticles observed

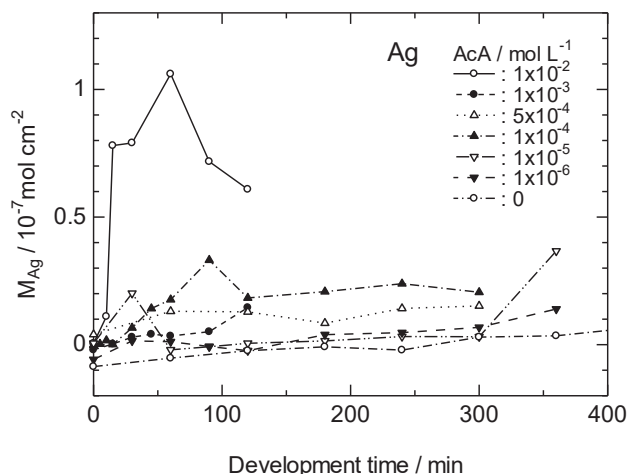


Fig. 4 Formation rate of silver amount formed on plate B measured with atomic absorption spectroscopy. The concentration of ascorbic acid (AcA) in the developer was altered from  $0$  to  $1 \times 10^{-2}$  mol/L, while that of Au(I) complex (AC) was fixed to  $1 \times 10^{-3}$  mol/L.

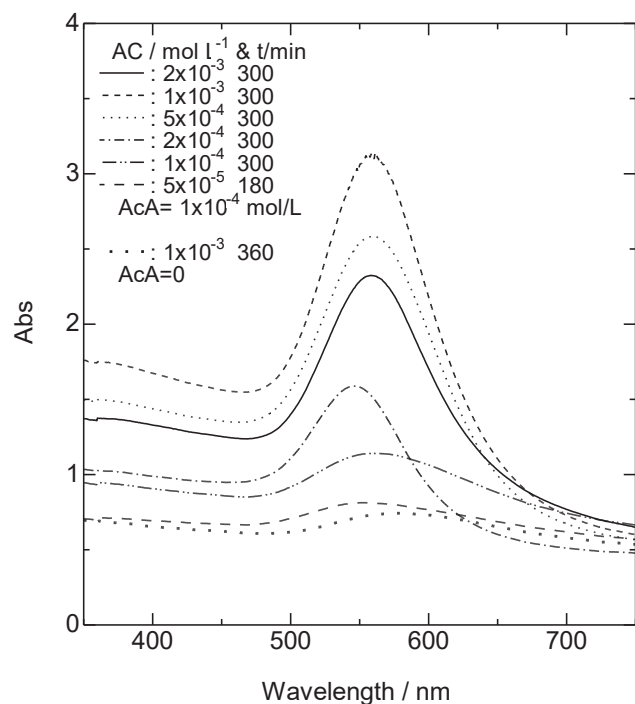


Fig. 5 Absorption spectra of gold nanoparticles formed on plate A at different concentrations of Au(I) complex (AC) from  $5 \times 10^{-5}$  to  $2 \times 10^{-3}$  mol/L in the developer. The concentration of ascorbic acid (AcA) was fixed to  $1 \times 10^{-4}$  mol/L. One sample with  $1 \times 10^{-3}$  mol/L AC and without AcA was included. The development time is presented with each legend.

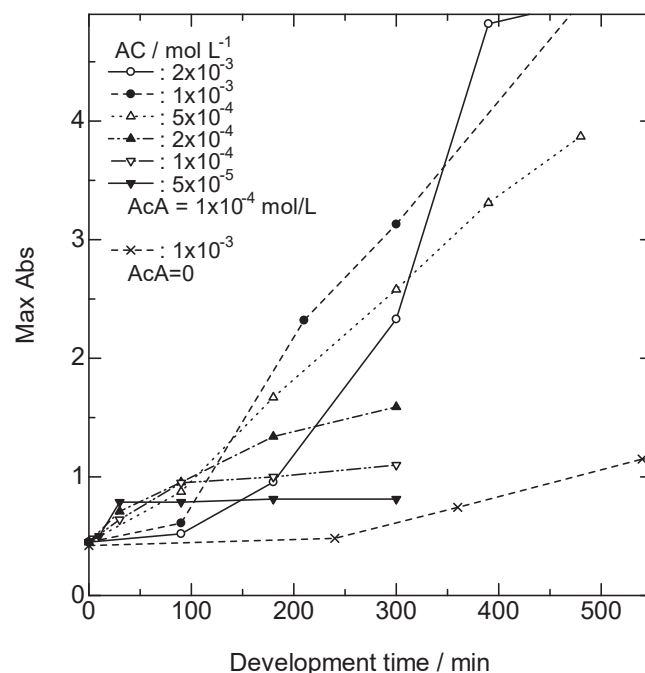


Fig. 6 Increasing rate of maximum absorbance in each spectrum of gold nanoparticles formed on plate A. The concentration of Au(I) complex (AC) in the developer was altered from  $5 \times 10^{-5}$  to  $2 \times 10^{-3}$  mol/L, while that of ascorbic acid (AcA) was fixed to  $1 \times 10^{-4}$  mol/L. One sample with  $1 \times 10^{-3}$  mol/L AC and without AcA was included.

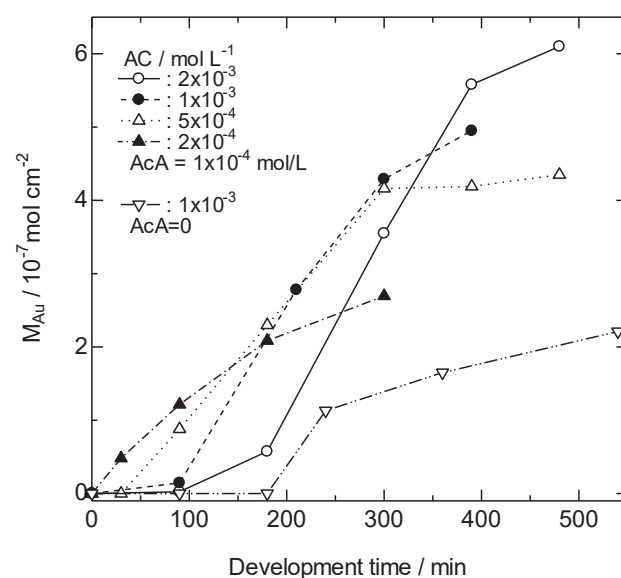


Fig. 7 Formation rate of gold amount formed on plate A measured with atomic absorption spectroscopy. The concentration of Au(I) complex (AC) in the developer was altered from  $5 \times 10^{-5}$  to  $2 \times 10^{-3}$  mol/L, while that of ascorbic acid (AcA) was fixed to  $1 \times 10^{-4}$  mol/L. One sample with  $1 \times 10^{-3}$  mol/L AC and without AcA was included.

from the electron micrographs is shown in Figure 8. There was no remarkable induction period and the growth rates were approximately the same each other. At a low AC concentration, the growth stopped at the stage where the diameter was small, although the size at saturation gradually increased with the AC concentration.

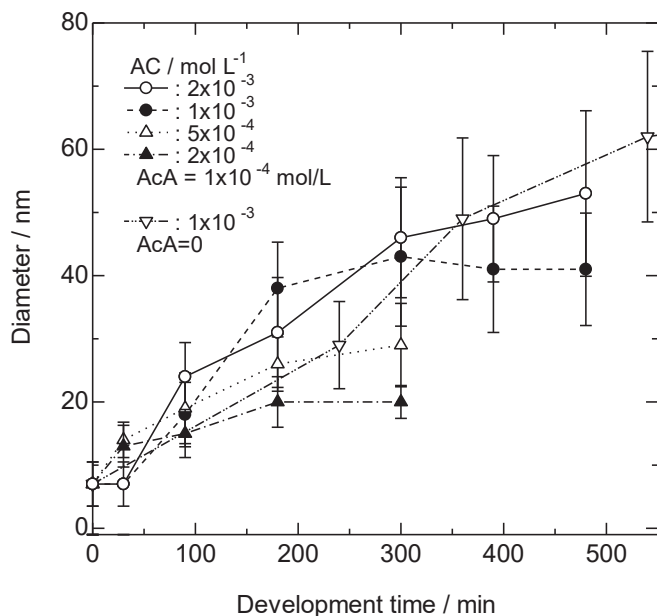


Fig. 8 Growth rate of diameter of gold nanoparticles formed on plate A measured from transmission electron micrographs. The concentration of Au(I) complex (AC) in the developer was altered from  $5 \times 10^{-5}$  to  $2 \times 10^{-3}$  mol/L, while that of ascorbic acid (AcA) was fixed to  $1 \times 10^{-4}$  mol/L. One sample with  $1 \times 10^{-3}$  mol/L AC and without AcA was included. The bar on each plotting point represents the standard deviation of the diameter.

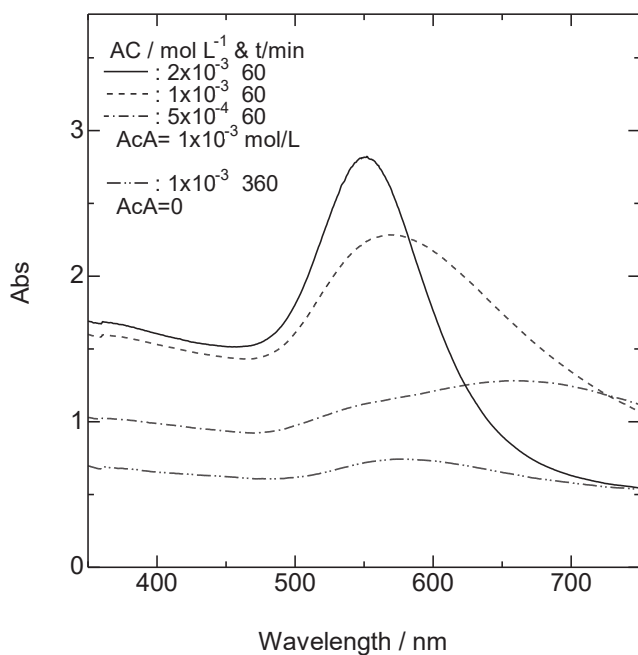


Fig. 9 Absorption spectra of gold nanoparticles formed on plate A at different concentrations of Au(I) complex (AC) from  $5 \times 10^{-5}$  to  $2 \times 10^{-3}$  mol/L in the developer. The concentration of ascorbic acid (AcA) was fixed to  $1 \times 10^{-3}$  mol/L, which was different from the condition in Figures 5–8. One sample with  $1 \times 10^{-3}$  mol/L AC and without AcA was included. The development time is presented with each legend.

When the AcA concentration was zero, the particle size did not exhibit saturation, and it increased continuously. From the perspective of the increase in particle size, the difference in the growth rates with and without AcA was not remarkable.

### 3.2.2 Ascorbic acid concentration of $1 \times 10^{-3}$ mol/L

This section presents the results when the AcA concentration was

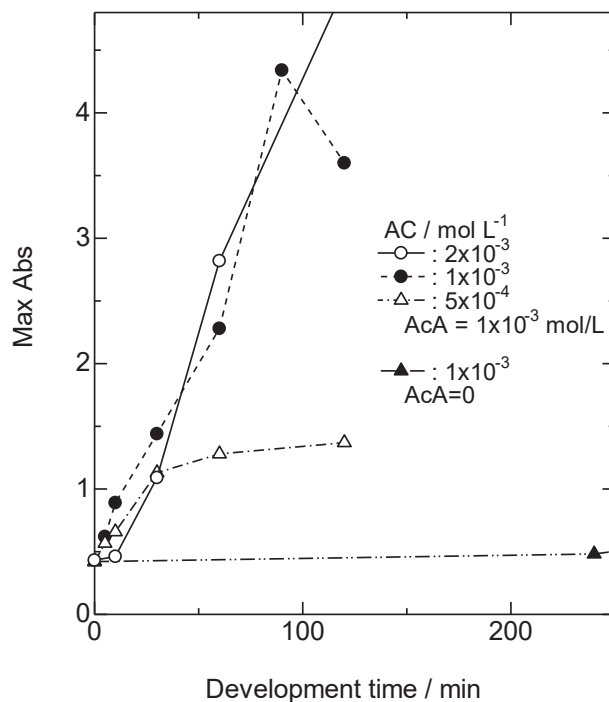


Fig. 10 Increasing rate of maximum absorbance in each spectrum of gold nanoparticles formed on plate A. The concentration of Au(I) complex (AC) in the developer was altered from  $5 \times 10^{-5}$  to  $2 \times 10^{-3}$  mol/L, while that of ascorbic acid (AcA) was fixed to  $1 \times 10^{-3}$  mol/L. One sample with  $1 \times 10^{-3}$  mol/L AC and without AcA was included.

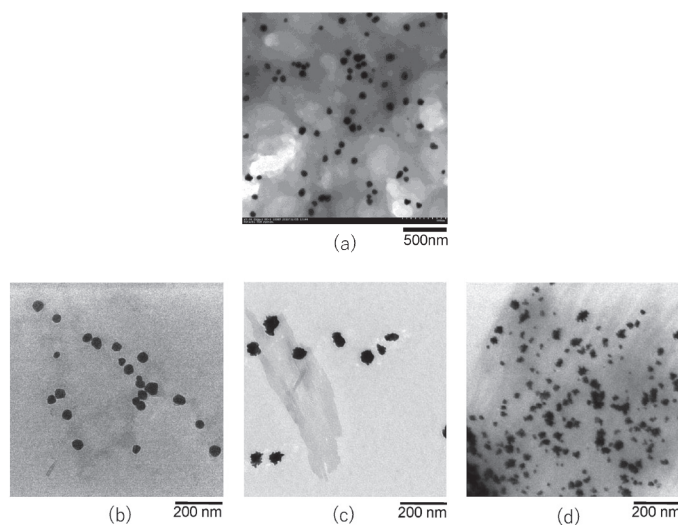


Fig. 11 Transmission electron micrographs of gold nanoparticles formed on plate A. The concentration of ascorbic acid (AcA) in the developer was set 0 for (a) and was fixed to  $1 \times 10^{-3}$  mol/L for (b) to (d), while that of Au(I) complex (AC) was altered as, (b)  $2 \times 10^{-3}$ , (a) and (c)  $1 \times 10^{-3}$ , and (d)  $5 \times 10^{-4}$  mol/L. The development time for (a) was 540 min and those for (b) to (d) were 120 min.



increased ten-fold to  $1 \times 10^{-3}$  mol/L. In this case, AC/AcA was set to small values less than two.

The dependence of absorption spectrum on the AC concentration is shown in Figure 9. When the AC concentration decreased, the wavelength of the absorption maximum shifted significantly to the long wavelength side and the band became broad. Figure 10 shows the dependence of increasing rate of maximum absorbance on the AC concentration. There was no remarkable induction period, and the rate difference was not evident for the case with AcA. Saturation of absorbance was observed at an AC concentration lower than the AcA Concentration.

The electron micrographs of gold nanoparticles are shown in Figure 11. At the highest AC concentration of  $2 \times 10^{-3}$  mol/L or without AcA, the surface of gold nanoparticle was smooth. Conversely, the surface became rough with decreasing AC concentration, and revealed many minute protrusions on the surface at an AC concentration of  $5 \times 10^{-4}$  mol/L. This behavior is the same as that reported previously<sup>8,9)</sup>.

The growth rate of the diameter of gold nanoparticles observed from the electron micrographs is shown in Figure 12. There was no evident induction period, and no significant difference in the rate for the case with AcA. Saturation of particle size was observed at the lowest AC concentration of  $5 \times 10^{-4}$  mol/L, and this result corresponded with the one in Figure 10. For the case without AcA, the growth rate was low, while the particle size increased continuously without saturation.

## Discussion

The following phenomena were observed in the formation process of gold nanoparticles when the AC and AcA concentrations were

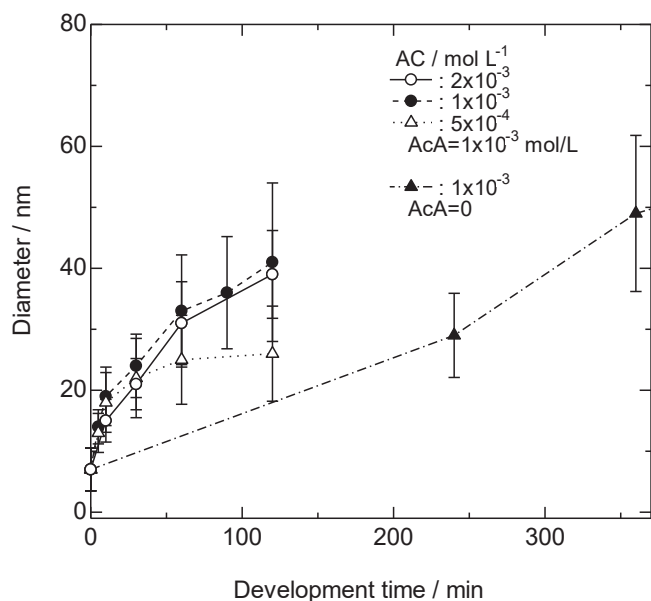


Fig. 12 Growth rate of diameter of gold nanoparticles formed on plate A measured from transmission electron micrographs. The concentration of Au(I) complex (AC) in the developer was altered from  $5 \times 10^{-5}$  to  $2 \times 10^{-3}$  mol/L, while that of ascorbic acid (AcA) was fixed to  $1 \times 10^{-3}$  mol/L. One sample with  $1 \times 10^{-3}$  mol/L AC and without AcA was included. The bar on each plotting point represents the standard deviation of the diameter.

altered:

- (I) The development rates of gold nanoparticles changed. The increasing rate of the absorbance and the formation rate of the gold amount changed significantly, while the growth rate of the particle size was not as pronounced.
  - (II) The induction period appeared at the initial stage of these rates. While the induction periods for the absorbance and gold amount exhibited similar behaviors, that for the particle size differed.
  - (III) The wavelength of the absorption maximum in the absorption spectrum shifted.
  - (IV) The absorption band width changed.
- In addition, the following phenomena, which were previously reported<sup>8,9)</sup>, were confirmed:
- (V) Silver atoms were produced simultaneously with gold atoms under some conditions.
  - (VI) The surface of the gold nanoparticles was usually smooth, but under some conditions, a rough surface with minute protrusions appeared.

These changes seem to depend on the concentrations of AC and AcA. However, it may be more probable that they depend on the concentration ratio of the two rather than on each concentration. To analyze this, we altered the concentration ratio of AC to AcA (AC/AcA) and examined the dependence of the above mentioned changes on this ratio.

The induction periods for the increasing rate of the maximum absorbance and the formation rate of the gold amount were analyzed. The period for increasing the absorbance from 0 to 0.05 and that for increasing the gold amount to  $2 \times 10^{-8}$  mol/cm<sup>2</sup> were estimated from the corresponding figures for the maximum absorbance and gold amount, respectively. These values were set as induction

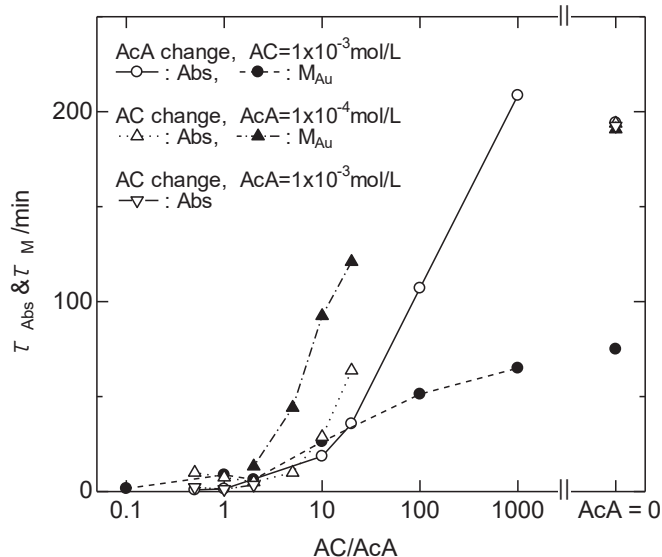


Fig. 13 Relationships between the concentration ratio of Au(I) complex (AC) to ascorbic acid (AcA) and the induction periods of the increasing rate of maximum absorption ( $\tau_{Abs}$ ) or the formation rate of gold amount ( $\tau_M$ ) for the series with altered AcA concentrations and a fixed AC concentration of  $1 \times 10^{-3}$  mol/L, and for the ones with altered AC concentrations and fixed AcA concentrations of  $1 \times 10^{-4}$  mol/L and  $1 \times 10^{-3}$  mol/L.

periods,  $\tau_{\text{abs}}$  and  $\tau_{\text{M}}$ . The relationships of  $\tau_{\text{abs}}$  and  $\tau_{\text{M}}$  with AC/AcA are shown in Figure 13, and indicated similar behaviors. The induction period was almost zero below the AC/AcA of unity, and significantly increased above the AC/AcA of two. These suggest that there is a boundary around the AC/AcA of unity.

Similarly, the relationships of the wavelength of absorption maximum  $\lambda_{\text{max}}$  with AC/AcA are shown in Figure 14. The wavelength also showed almost the same behavior at the AC/AcA of approximately unity. When the ratio was unity or less,  $\lambda_{\text{max}}$  increased significantly indicating that the peaks shifted to a long wavelength region. The values of  $\lambda_{\text{max}}$  for the AC concentration of  $1 \times 10^{-4}$  mol/L presented by the black circles were uncertain, because they were obtained from spectra with a small absorbance.

Both figures show that substantial changes occurred at the AC/AcA of approximately unity. Meanwhile, the formation of silver atoms was observed, as shown in Fig. 4, for AC/AcA=0.1. The surface of the gold nanoparticles shown in Figure 11 changed from smooth to rough at the AC/AcA of approximately unity. These changes suggested that the formation mechanism of gold nanoparticles changed in the region where the AcA concentration was higher than the AC concentration.

However, upon comparing with the case without AcA, the formation rate of gold amount with AcA was high even at an AcA concentration of  $1 \times 10^{-6}$  mol/L, which was 1/1000 of the AC concentration, as shown in Figure 3. The mechanism may differ in the cases with and without AcA.

From these results, we can consider that there are three processes for gold nanoparticle formation from a viewpoint of AcA/AC.

- (1) In the case that there is no AcA and only AC: The rates of increase in the absorbance and formation of gold amount were low, and there was an induction period in the rates measured with the maximum absorbance and the gold amount, while the induction period for the particle size was small or insignificant. The absorption spectrum had a slightly sharp band and absorp-

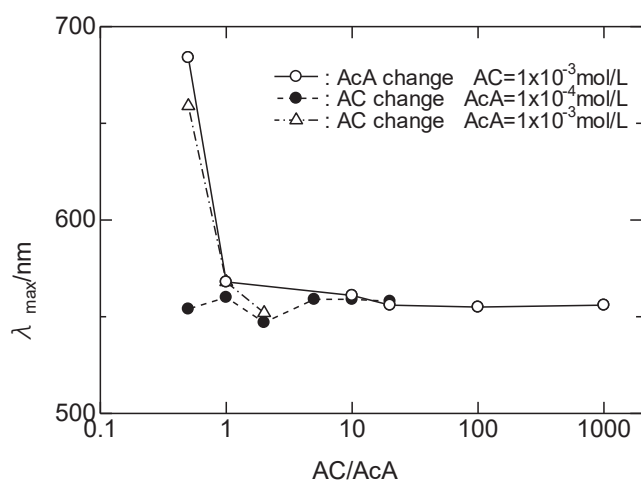


Fig. 14 Relationships between the concentration ratio of Au(I) complex (AC) to ascorbic acid (AcA) and the wavelength at the absorption maximum for the series with altered AcA concentrations and a fixed AC concentration of  $1 \times 10^{-3}$  mol/L, and for the ones with altered AC concentrations and fixed AcA concentrations of  $1 \times 10^{-4}$  mol/L and  $1 \times 10^{-3}$  mol/L.

tion occurred in the green spectral region.

- (2) In the case that the AcA concentration is smaller than the AC concentration: Particles with only gold atoms were formed. The increasing and formation rates were higher than that in the absence of AcA, but it had the induction period. The absorption spectrum had a sharp band and absorption occurred in the green spectral region.
- (3) In the case that the AcA concentration is larger than the AC concentration: Gold particles contained a small amount of silver atoms. The increasing and formation rates were high and there was no induction period. The band in absorption spectrum was broad and shifted to the longer-wavelength side of the red spectral region.

Therefore, we can relate these three cases to the following three formation processes of gold nanoparticles:

- (A) no AcA: Disproportionation reaction of AC.
- (B) The AcA concentration is smaller than the AC concentration: Direct reduction of AC by AcA. This process may be predominant in the reduction of silver halide by AcA, but the rates must be low.
- (C) The AcA concentration is larger than the AC concentration: Simultaneous reductions of AC and silver halide by AcA. The reduction of AC may be still predominant; however, excess AcA can rapidly reduce silver halide.

Processes (A) and (B) proceed with the catalytic action of LISs. As already reported<sup>7-9)</sup>, the required minimum number of silver atoms in LIS for catalytic activity differs between the disproportionation reaction of AC and the reduction of AC by AcA. The former reaction is catalyzed only by LIS of large size. Therefore, the number of gold nanoparticles generated with process (A) becomes less than that with process (B), thereby causing a decrease in the maximum absorbance and gold amount in process (A).

The reaction rate of process (B) was low despite process (B) being the predominant reaction.

A possible explanation is as follows: AC and AcA both form a certain complex of monovalent gold ion Au(I) quickly, and approximately all AcA is consumed owing to excess AC. This complex decomposes into a gold atom through the catalytic action of LIS, although the decomposition may be slow. After LIS is embedded in these gold atoms, following decomposition of the complex proceeds through similar catalytic action of gold atoms in the particles. This activity may be similar to that of silver atoms in LIS and the development rate of gold deposition will be low.

The amount of silver atoms produced with process (C) was less than that of gold, even though the amount of AcA was significantly in excess. An explanation is the larger ionization tendency of silver, but there is another possibility that most of the silver atoms would react with the AC complex and form silver halide again according to the following formula:



The formation of silver atoms by the reduction of silver halide with AcA catalyzed by LIS is similar to a normal development process. Therefore, the reaction rate to form silver atoms by AcA may be

high and significant amount of silver atoms is formed. The formation of gold atoms through the reaction in Eq. (1) proceeds quickly, because the silver atoms react directly with the gold ion complex without any catalyst. This accelerates the reaction of gold deposition with process (C) and the induction period disappears.

When the process of Eq. (1) proceeds, a mixture of gold atoms and silver halide is formed. However, as this silver halide is removed through fixation following the development, gaps will be generated on the particle surface by this removal, and the surface will become rough, as shown in Fig. 11(c). The silver atoms detected with atomic absorption spectroscopy are the residues embedded inside the particle, and the amount of silver becomes small.

Because LIS is composed of silver atoms, it is also possible that silver atoms in LIS form gold atoms by Eq. (1) instead of the embedding by gold atoms. However, as the amount of silver atoms in LIS is very few, the gold particles formed are also very small.

One possible reason why the wavelength of the maximum absorption in the absorption spectra shifts to a longer-wavelength region and the bands becomes broad with process (C) may be that silver atoms are included in the particles, thereby changing the wavelength of the localized surface plasmon resonance. Another reason may be that the shape of the particles changes differently through the reaction of Eq.(1), which affects the wavelength of plasmon resonance.

The behavior of the induction period evaluated with the particle size was different from that evaluated with the absorption spectrum or the gold amount. This is explained as follows: We measured the absorbance or the gold amount for all gold particles together, while we evaluated the diameter for each particle individually. The size distribution of the gold particles was fairly wide, as shown in the electron micrographs in Figure 11 or in the standard deviation of the diameter in Figures 8 and 12. This suggests that the rate of particle growth differs widely. Meanwhile, the diameter observed with the electron microscope was not zero, but approximately 7 nm at the development time of zero, as shown in Figures 8 and 12. It was explained in a previous report<sup>8)</sup> that these were LISs of large size owing to the large exposure value, and were larger than the resolution of an electron microscope. Because a large LIS had a higher development rate, we only observed the growth behavior of large and evident particles at the initial stage of development and measured the diameters of these particles only. This will apparently diminish the induction period measured with the particle size. Because the smaller LISs had a low development rate, the gold particles formed on the small LISs were not observed with the electron microscope at the initial stage, while they contributed to the absorption spectrum and gold amount.

The particle size was unsaturated without AcA, while it saturated at a low AcA concentration for the same AC concentration. The number of LISs to catalyze the disproportionation reaction is less than that to catalyze the reduction of AC by AcA<sup>7-9)</sup> owing to the difference in LIS sizes. Because the number of gold particles formed without AcA becomes few, the amount of usable AC for the growth of each particle increases and these gold particles can continue to grow without saturation.

## Conclusion

1. The reaction whereby gold nanoparticles were formed with the gold deposition development depended not only on the concentrations of AC and AcA but also on the concentration ratio of both solutions.
2. Gold atoms were formed by the disproportionation reaction of monovalent gold ions in AC without AcA. The reaction rate was low and had a significant induction period.
3. When the AC concentration was larger than the AcA concentration, the reduction of AC by AcA proceeded. This reaction rate was higher than that in the disproportionation reaction, but the induction period was still considerable.
4. When the AcA concentration increased and AC/AcA became less than unity, the reaction rate increased remarkably and the induction period disappeared. In this case, AcA produced silver atoms simultaneously by reducing silver halide.
5. It is suggested that the reaction between these silver atoms and gold ions will form gold atoms and silver halide. This reaction proceeds quickly and increases the development rates. Because the formed silver halide is removed through subsequent fixation, the particle surface becomes rough. This also causes the shift of the absorption peak, as well as band broadening.

## Acknowledgment

The authors thank Konica-Minolta Company for providing the ultra-fine-grain emulsion used as plate A in this study. The authors received immense support with using the atomic absorption spectrometer from the Center for Analytical Instrumentation in Chiba University, and would like to express their gratitude to Dr. Mass in this Center, as well as Dr. Okawa at the Graduate School of Engineering in Chiba University for their extensive support. The authors also thank Dr. Shiba at the Graduate School of Engineering and Ms. Tachiki of the Faculty of Engineering in Chiba University for their valuable assistance and guidance with using the electron microscope.

## Footnote

\* Previously we reported that the exposure time of this flash lamp was  $10^{-6}$  s. This was because the performance of the lamp had been informed as such. However, recent measurement has indicated it to be  $10^{-3}$  s. It is speculated that  $\mu$  (micro) seconds and m (milli) seconds had been confused.

## References

1. K. Kuge, M. Arisawa, N. Aoki, A. Hasegawa, *Jpn. J. Appl. Phys.*, **39**, 6550 (2000).
2. K. Kuge, K. Kimijima, M. Arisawa, N. Aoki, A. Hasegawa, *J. Soc. Photogr. Sci. Technol. Jpn.*, **64**, 242 (2001) (in Japanese).
3. K. Kuge, K. Suzuki, N. Aoki, A. Hasegawa, *J. Soc. Photogr. Sci. Technol. Jpn.*, **65**, 536 (2002) (in Japanese).
4. K. Kuge, M. Arisawa, N. Aoki, A. Hasegawa, *Imaging Sci. J.*, **52**, 176 (2004).



5. K. Kuge, T. Nakao, S. Saito, O. Hikosaka, A. Hasegawa, *J. Imaging Sci. Technol.*, **51**, 96 (2007).
6. K. Kuge, X. Chen, T. Sakai, A. Hasegawa, *J. Imaging Sci. Technol.*, **54**, 010507 (2010).
7. K. Kuge, Y. Yu, K. Fuma, R. Ito, T. Sakai, *Bull. Chem. Soc. Jpn.*, **84**, 947 (2011).
8. K. Kuge, H. Tomimatsu, F. Shiba, *Bull. Soc. Photogr. Imaging Jpn.*, **26**, 23 (2016).
9. K. Kuge, T. Adachi, H. Tomimatsu, *J. Soc. Photogr. Imaging Jpn.*, **81**, 41 (2018) (in Japanese).
10. D.C.Birch, G.C.Farnell, R.B.Flint, *J. Photogr. Sci.*, **23**, 249 (1975).
11. S. Jablonka, C. Mora, P. M. Nowak, A. Zaleski, *J. Information Recording*, **23**, 249 (1996).
12. A.C.Reeder, H.E.Spencer, *J. Imaging Sci.*, **31**, 126 (1987).
13. K. Kuge, T. Tsutsumi, K. Morimoto, S. M. H. Kimura, T. Suzuki, T. Mitsuhashi, A. Hasegawa, *J. Imaging Sci. Technol.*, **53**, 010507 (2009).
14. K. Kuge, T. Inaba, S. Suzuki, S. Kodaira, *J. Soc. Photogr. Imaging Jpn.*, **79**, 376 (2016) (in Japanese).
15. K. Kuge, K. Morimoto, *Bull. Soc. Photogr. Imaging Jpn.*, **27**, 1 (2017).